

DYNAMIC ANALYSIS OF CABLE LOSS OF A CONCRETE-FILLED STEEL TUBULAR ARCH BRIDGE

Q. Wu, B. Chen, J. Zheng, Y. Yu

College of Civil Engineering, Fuzhou University, Fuzhou, Fujian, CHINA.

e-mails: 18606936436@163.com, chen-kang-ming@163.com, wuqingx@fzu.edu.cn

SUMMARY

Based on concrete-filled steel tubular (CFST) arch bridge, the finite element (FE) model was built with the ANSYS/LS-DYNA software. The process of cable loss was simulated with the contact-impact method to analyze the variation of the internal forces of different structure members before and after cable loss. The results show that cables, arch ribs and deck slabs are all influenced by the impact produced by the process of cable loss. Among them, the influence of cable loss on the adjacent cables is the largest and the variation of axial force can exceed three times of the initial force. Therefore, the effect of dynamic force, which is far greater than the static response during the cable loss, should be considered. It is also concluded that the influence of cable loss on the main girder is significantly greater than that on the arch ribs. The local collapse of floor system can be found due to the insufficient strength of the weld connection between the transverse and longitudinal beams.

Keywords: *CFST truss arch bridge, K-joint, stress concentration factor, ratio of chord diameter to thickness, ratio of chord diameter to brace diameter, ratio of chord thickness to brace thickness, angle between chord and brace.*

1. INTRODUCTION

In the half-through or through arch bridges, the deck is suspended from the arch ribs (arch ring) by a number of cables, through which the dead and live loads that act on the deck can be transmitted to the arch ribs [1-2]. Given the important role of cables in the load-carrying properties of arch bridge, its reliability and durability are of vital importance for the safety and normal service of bridge. However, cables are known to be highly vulnerable to damage caused by explosion, bumping, fire or lightning, which will lead to the collapse of floor system or even local or internal failure of arch ribs. Such tragic events are by no means unusual. For instance, Xiaonanmen Bridge, an reinforced concrete rib arch bridge over the Jinsha River in Yibin city of Sichuan Province, underwent cable failure and then collapse of floor system of about 30 m on November 7, 2001. Other examples included the rupture of the second cable of Kongque River Bridge in Kuerle of Xinjiang Uygur autonomous region on April 12, 2011, which resulted in the falling of the third, fourth and fifth beams into the river, and collapse of pavement of about 10×20 m; and the cable failure of the Gongguan Bridge in the Wuyi Mountain City of Fujian Province on July 14, 2011, which resulted in the collapse of plate beams [3-4].

Disproportionate collapse of a structure has been a topic of considerable research, most of which has been directed to buildings rather than bridges. So far, a number of design guidelines have been developed in some countries, such as Great Britain, European Union, and United State [5-8]. In the design of cable-stayed bridges, sudden rupture of cable is considered by removing one cable from the analysis, and the internal force and deformation of beam are limited [9]. However, no similar analysis has been undertaken for arch bridges, and it is analyzed in a static rather than dynamic way. In this study, the cable loss of a Rigid-frame tied through CFST arch bridge was simulated using ANSYS/LS-DYNA. We compared the changes in the internal forces of the primary components of arch bridge in response to the rupture of two short and long cables, and discussed potential failure mode of the bridge.

2. ARCH BRIDGE TO BE MODELED AND FE MODEL (FEM)

2.1. Arch bridge

A Rigid-frame tied through CFST arch bridge is considered, as schematically shown in Fig 1, where the calculation span length is 150 m, the rise-to-span ratio is 1/4.5, the arch axis is a catenary with a coefficient of 1.167 [10]. There are two CFST truss arch ribs, the cross section of which is 2.0 m in width and 3.0 m in height, and composed of four chords of $\Phi 750 \times 12$ mm steel tubes, lateral bracing of $\Phi 400 \times 10$ mm steel tubes, and web plates of $\Phi 245 \times 10$ mm steel tubes. All the steel tubes are filled with C50 micro-expansion concrete. At the arch springing, the upper and lower chords are connected by web plates instead of steel tubes to improve the local stiffness of arch ribs. There are a total of 17 pairs of cables spaced at an interval of 8.0 m for each arch, and twin cables spaced 48 cm apart are used with adjustable cold-heading anchorages at both ends, as shown in Fig 2. The cables are made of high tensile strength wires ($61\Phi 7$) and covered with double high density polyethylene coating. Sixteen high-strength low-relaxation prestressed strands ($12 \times 7\Phi 5$ mm) are equipped as tied bars to balance the thrust for each rib, each having a standard strength R_{yb} of 1680 MPa, and protected in the same way as the cables. The tied bars are positioned outside the anti-crash barrier under the arch rib, pass through the arch rib at springing and are anchored outside the cap beam. There are totally 17 transverse prestressed concrete box beams, which are the primary load-carrying members of the floor system and connected by 36 longitudinal stiffened box beams. The longitudinal beam is made of Q345 steel, and both top and bottom plates are 10 mm thick. The deck is a simply supported continuous system and made of precast hollow slabs, it is interconnected with the transverse beams by shear keys.

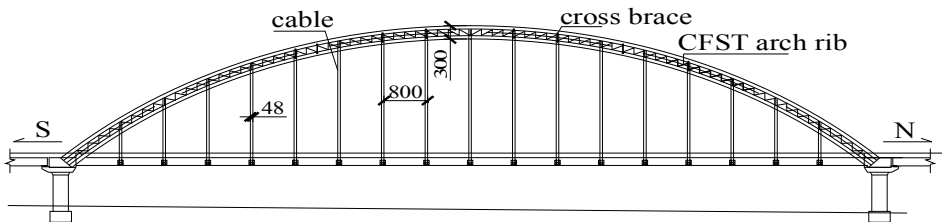


Fig. 1. General arrangement of the Rigid-frame tied through CFST arch bridge (unit: cm).

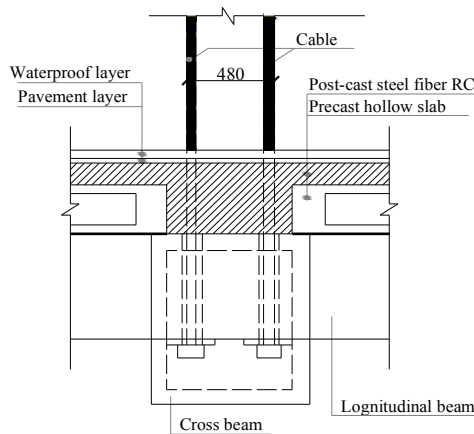


Fig. 2. Structure diagram of cable joint (unit: cm).

2.2. FE Model

A three-dimensional FEM was developed using ANSYS/LS-DYNA, the arch rib, transverse and longitudinal beam, bracing, web plate and deck were simulated by beam161, and the cable and tie bar by Link167 (an explicit tension-only spare). The arch rib was simulated with 688 elements using double-element method, and the floor system with 396 elements using beam-grid method. The stiffness of bridge deck was distributed to the transverse and longitudinal beams according to the effective width, and weight was distributed to the nodes of deck in the form of concentrated force. The stiffness of pavement was not considered, but its weight was included in the bridge deck. The boundary conditions were set according to the actual support condition of the bridge. The node coupling method was applied to simulate the principal and subordinate relationship of the cable bottom end nodes with the longitudinal beam nodes and arch springing with arch rib. The four arches springing were constrained by rigid joint, and six direction freedoms of nodes were constrained. The transverse and longitudinal beams and cables formed a suspended system, and the floor system would not bear the tension force. The longitudinal constraint between longitudinal beam and cap-beam was released, and the horizontal thrust of arch rib was balanced by the tie bars.

2.3. FEM verification

A field load test was conducted on the bridge using seven heavily loaded three-axle dump trucks, each being approximately 350 kN, to provide the design live load for the test. Three conditions were considered: maximum negative bending moment at the south springing (case 1), maximum positive bending moment at the south L/4 rib (case 2) and arch crown (case 3). We measured rib deflections and strains of some key components.

A comparison was made between the test and FEM results for the three cases. Tab. 1 shows that there is only a less than 15% difference in strains at the top and bottom sides of arch rib, Fig. 3 shows a consistent agreement in the deflection, with a difference of less than 15%, and Tab. 2 also shows that there is a marginal difference in the fundamental frequencies. It therefore can be concluded that FEM is reliable.

3. DYNAMIC ANALYSIS METHOD OF CABLE LOSS

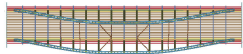
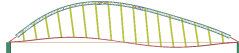
3.1. Simulation method

Cable loss could cause disproportionate collapse of the bridge structure, which underscores the need to consider the dynamic response of the structure in the analysis of disproportionate collapse. However, it is known that this phenomenon is not caused by the dynamic load on the structure, as in this case, the structure is not subjected to any specific dynamic load except the impact load due to the collapse of the component, thus the original dynamic response of the structure is caused by component vibration as a result of the geometric catastrophe. This is where the essential difference lies between the dynamic calculation for disproportionate collapse and normal dynamic calculation. The key to this problem is to accurately simulate the cable loss to make the dynamic response of structure come nearer the truth [11].

Table 1. Comparison of strains between the test and FEM results (unit: $\mu\epsilon$).

Load cases		Case 1 & 2		Case 3	
	Section	Test	FEM	Test	FEM
Crown	Top side	29.8	23.3	-76.8	-94.7
	Bottom side	-42.5	-34.9	73.0	98.7
L/4	Top side	-77.3	-96.9	14.8	19.6
	Bottom side	81.5	96.6	-45.3	-45.7
Springing	Top side	85.3	94.6	—	—
	Bottom side	-108.0	-112.8	—	—

Table 2. Comparison of principal modal.

Order	Test frequency (Hz)	Calculation frequency (Hz)	Modal shape
1	0.4	0.358	
2	0.7	0.746	

The contact-impact interface algorithm in the ANSYS/LS-DYNA was used to simulate the dynamic process of cable loss. The internal force of flexible cables subjected to lateral collision will increase to a high level within a short time by increasing the velocity of collider, which will cause disturbance and vertical impact on the arch rib and floor system. The cables will break when the internal force exceeds a critical value, this is equivalent to impose a corresponding impact in the opposite direction of the cable force.

The collider was simulated with solid elements in this study, in which its contribution to the kinetic energy was considered, without considering its interaction with bridge deck.

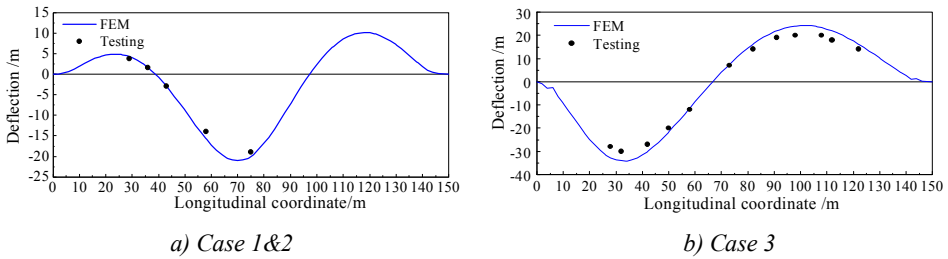


Fig. 3. Deflection curve of arch rib.

In the simulation, the weight and velocity of the collider were controlled to enable the cable to reach the corresponding internal force, and the collider was assumed to be in one sided contact with the cable. In this way, the analytic program will automatically determine the contact surface in the model. The restart mode was adopted in this study, including (1) small restart: A small restart was used when a minor change to the K file (Solution File) was necessary, with which we could modify output time interval of destination files, reset the computation time, remove contacts and units, modify speeds, boundaries and loading conditions, convert rigid body to deformable body, as well as modify some control parameters; and (2) full restart: A full restart was appropriate when extensive modifications to the K file were required, with which we could add new materials, PART and contact definition, change curve, define damping and some control parameters. A full restart can be considered as a totally new analysis, except that it inherits the shape and stress information relevant to PART from the original analysis, which will be used as the initial conditions for the next full restart. In this study, the small restart was used to apply initial velocity to the collider and delete elements, while the full restart was used to initialize deformation and stress after the model modification. They were used alternately to complete the whole simulation process, as shown in Fig. 4.

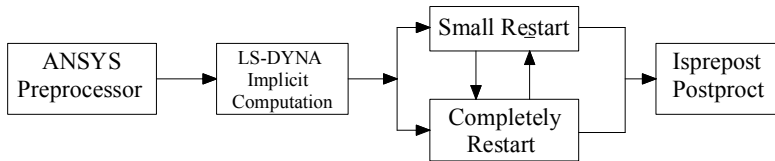


Fig. 4. Simulation process of the cable failure.

Plastic Kinematic model of Material 3 in ANSYS/LS-DYNA is used to simulate the cable constitutive model, as shown in Fig. 5. The fundamental formula of this model is [12]

$$\sigma_y = [1 + (\varepsilon/C)^{1/p}](\sigma_0 + \beta E_p \varepsilon_{eff}^p) \quad (1)$$

Where σ_0 is the initial yield strength(condition yield), ε is the strain rate, ε/C is the strain rate parameter, ε_{eff} is the effective plastic strain, and E_p is the plastic hardening modulus.

With the Plastic Kinematic constitutive model, the cables could be ruptured by setting the value of critical strain. The internal force time-history curve of the cable subjected to lateral collision is shown in Fig. 6. The plastic damping matrix is treated as Rayleigh damping matrix in the dynamic analysis, with a damping ratio of 0.05.

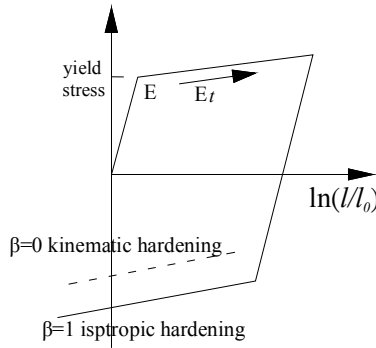


Fig. 5. Constitutive relation of Plastic Kinematic modal.

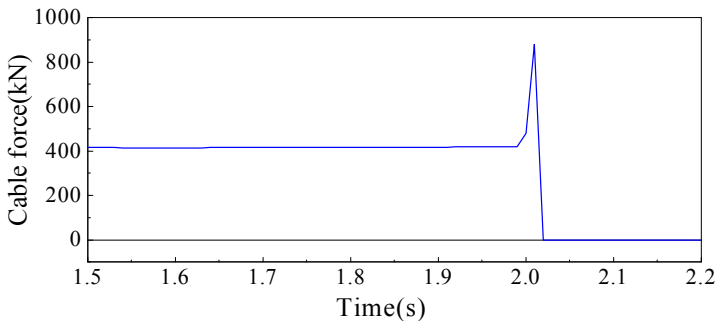


Fig. 6. Time-history curve of cable force.

3.2. Selection of ruptured cables

The long and short cables will have almost the same force under dead load. However, the short cables are at a more disadvantageous position as they are closer to the junction of suspended and supported deck, where the arch rib displacement induced by load and temperature and floor system displacement induced by temperature are concentrated. Thus we first focus on the impact of short cable loss. There are totally 68 cables, which are numbered in consecutive order from 1# to 34# on the upstream side, and from D1# to D34# on the downstream side. Those cables at the most disadvantageous load are selected for further analysis. The ultimate load carrying capacity is analysed according to the basic combinations of load effect (1.2 dead load + 1.4 trailer load), and the corresponding internal force of cables are shown in Fig. 7 (Only 17 cables because of symmetry). It shows that 3# and 4# cables have the largest internal force, which will be selected as the representative of the short cables, and we also selected 13# and 14# cables as the representative of the long cables.

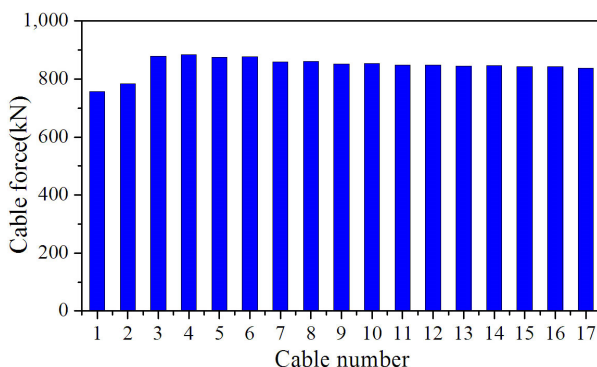


Fig. 7. Cable force under the combination of dead and trailer load.

4. THE FORCE CONDITIONS OF THE BRIDGE WITH SHORT CABLES LOSS

4.1. Cable

The axial force of 1#, 2#, 5#, and 6# cables that are adjacent to the ruptured cables change most obviously in response to the loss of 3# and 4# cables, as show in Fig. 8. The maximum axial force is 1421 kN and 1546 kN for 1# and 2# cables, respectively, which occurs in about 0.13 s after cable loss, and it is 1225 kN and 1143 kN for 5# and 6# cables, which occurs in about 0.11 s after cable loss. Thus cable loss seems to have the most significant influence on the adjacent cables, and their axial force is over 3 times the initial force. It is therefore necessary to consider the effect of dynamic force that is far greater than the static response during the cable loss. In addition, the loss of 3# and 4# cables causes a significant displacement of the deck close to D3# and D4# cables, which make the axial force of D3# and D4# cables be as high as 900 kN. The other cables far away from the ruptured cables are less affected, and the maximum axial force is less than 700 kN.

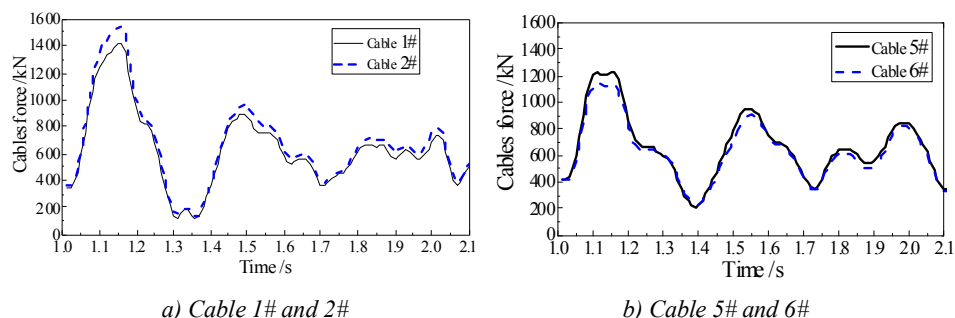


Fig. 8. Time-history curve of adjacent cable force under the short cables loss.

4.2. Arch rib

The time-history curve of arch rib and transverse beam due to loss of 3# and 4# cables are shown in Fig. 9. In contrast to the dramatic variation of displacement of beams, the arch rib shows a much more smooth variation. Thus cable loss has a more significant influence on the beams than the arch ribs.

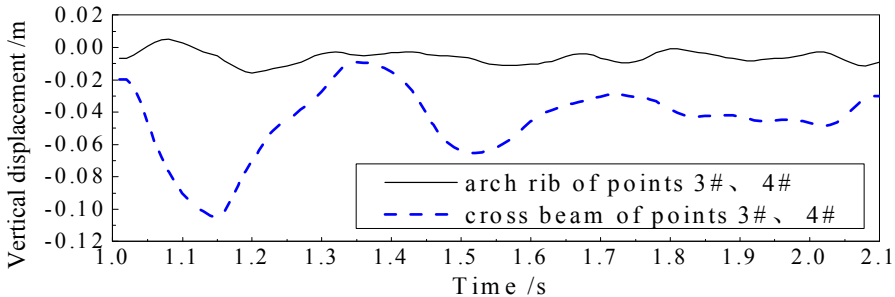


Fig. 9. Time-history curve of arch rib and cross beam under the short cables loss.

When the displacement at the suspension point of ruptured cables reaches the maximum value ($t = 1.08$ s), the internal force of arch springing, L/4 and crown on both sides are shown in Tab. 3, and the time-history curve of L/4 is shown in Fig. 10. It shows that the axial force of arch rib increases slightly, while the bending moment remains almost unchanged. The axial force of upper chord of L/4 decreases at first and then increases, while the opposite appears to be the case for the lower chord. A similar pattern is observed for the arch rib at mid-span.

4.3. Floor system

The transverse and longitudinal beams are connected by first class welding. We primarily focus on the force at the welding point, which is considered to be the weakest point of the steel structure. Fig. 11 show the time-history of W2 and W3 (weld numbers are shown in Fig. 12) in response to the loss of 3# and 4# cables. It shows that the moment at W2 and W3 increases sharply to 3204 kN.m and 3118 kN.m, respectively, and the shear force changes symmetrically by about ± 1500 kN. The moment-time curve and shear force-time curve at W1 and W4 are also analyzed. As compared with W2 and W3, the internal forces at W1 and W4 are relatively smaller, the moment and shear force are 1823 kN.m and 645 kN at W1, and 1429 kN.m and 554 kN at W4, respectively. The tensile resistance capacity of welding is calculated according to the Code for design of steel structures, and the results are shown in Tab. 4. It indicates that the stress at W2 and W3 exceeds the tensile resistant capacity, thus the longitudinal beam would be damaged due to insufficient strength of connection, leading to a large vertical displacement of the transverse beam and bridge deck, and then local collapse of the floor system.

4.4. The failure mode of arch bridge

It follows from the above analysis that the other cables are unlikely to break as their axial forces will not exceed the allowable stress under short cable loss, and the arch rib is also less affected thanks to the smooth variation in the internal forces. The transverse beam and floor system would probably have local collapse due to insufficient connection strength between the transverse and longitudinal beams. Thus the potential failure mode of bridge is the local collapse of floor system, as shown in Fig. 13.

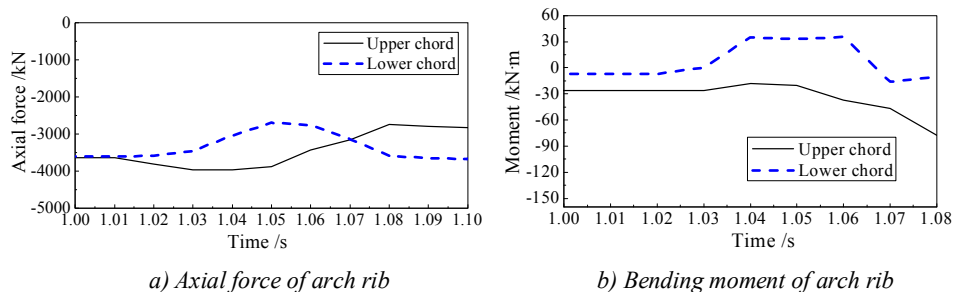


Fig. 10. Time-history curve of L/4 section under the short cables loss.

Table 3. Arch rib force pre-and post the short cables loss.

No.	Position	Upstream side				Downstream side			
		Axial force (kN)		Moment (kN·m)		Axial force (kN)		Moment (kN·m)	
		Before	After	Before	After	Before	After	Before	After
1	Springing	-18322	-16769	-653	-653	-18322	-17810	-653	-653
2	Upper chord of L/4	-3638	-3973	-26	-18	-3638	-3661	-26	8
3	Bottom chord of L/4	-3606	-2696	-7	35	-3606	-3348	-7	37
4	Upper chord of crown	-3659	-3955	148	162	-3659	-3666	148	152
5	Bottom chord of crown	-3012	-2728	97	116	-3012	-3001	97	102

Table 4. Result of the welds strain and strength under the short cables loss.

Weld number	W1	W2	W3	W4	Resistance capacity
Stress (MPa)	123.0	222.8	216.9	97.2	200

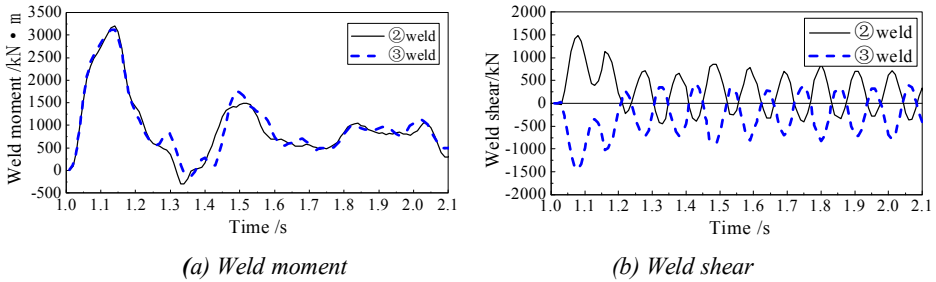


Fig. 11. Time-history curve of weld force under the short cables loss.

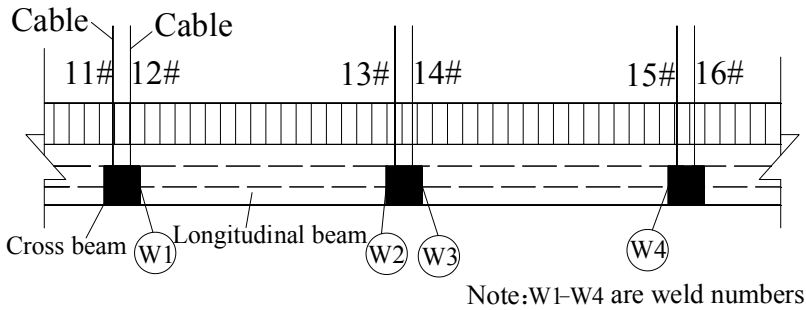


Fig. 12. Weld number of longitudinal beam.

5. FORCE CONDITIONS OF STRUCTURE UNDER LONG CABLES LOSS

Force conditions of structure under long cables loss is also analyzed by the same calculation method, and the results showed that the failure mode of bridge structure is as same as the condition of short cable loss. The transverse beam and floor system would probably have local collapse due to insufficient connection strength between the transverse and longitudinal beams. Thus the potential failure mode of bridge is the local collapse of floor system, as shown in Fig. 14.

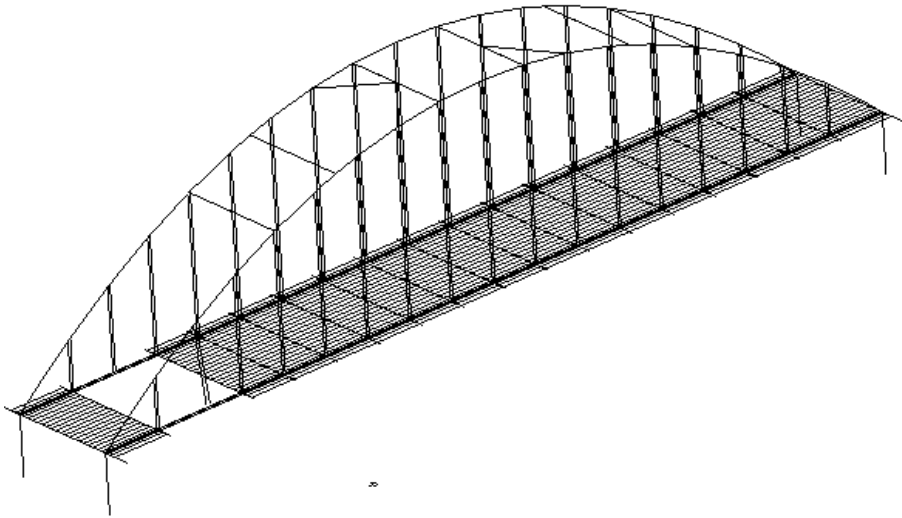


Fig. 13. Failure mode of arch bridge with short cable loss.

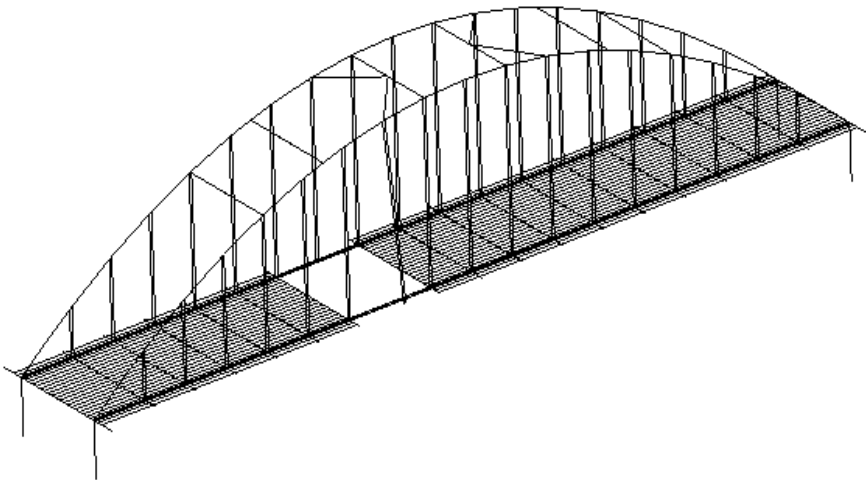


Fig. 14. Failure mode of arch bridge with long cable loss.

6. CONCLUSIONS

A FE model of a Rigid-frame tied through CFST arch bridge was constructed using ANSYS/LS-DYNA software, which was verified to be reliable by the results of dynamic-static load test. The loss of two short and two long cables were simulated using contact-impact method, and the dynamic analysis of bridge structure before and after

cables loss was carried out. The results show that cable loss has the most significant influence on the adjacent cables, and the axial force is over 3 times the initial force. It is therefore necessary to consider the effect of dynamic force that is far greater than the static response during the cable loss. It is also concluded that cable loss has a greater impact on the transverse beams than the arch ribs. As a result, the floor system would have local collapse due to insufficient connection strength between the transverse and longitudinal beams. In this study, we also discussed the simulation method and dynamic response to cable loss. Findings from this study will provide some reference for the design of CFST arch bridges.

However, how to simplify the dynamic response of cable loss to static response and improve the disproportionate collapse resistance by means of constitution design requires further research.

REFERENCES

- [1] CHEN, B.C., 2007, *Concrete Filled Steel Tubular Arch Bridges (Second Edit)*, Beijing, China Communications Press.
- [2] WEI, J.G & CHEN B.C., 2004, Finite element methods for analysis on material nonlinearity of concrete - filled steel tubular arch, *Journal of Fuzhou University (Natural Science)*, 32(3), pp. 344-348.
- [3] GUO, Z.L., 2010. *Analyze on the Process of Suspender's Fracture and Research on the Safety Countermeasure*, Fuzhou, Fuzhou University master's thesis.
- [4] ZHANG, X.C. 2002. Analyzing the reason and renovating project of "little south door Jinsha River bridge of Yibin City" collapsing, *Journal of Henan Urban Construction Junior College*, 11(2), pp. 15-17.
- [5] British Standard Institute, *Structural Use of Concrete: (Part 1)*, Code of Practice for Design and Construction, 1997.
- [6] European committee for standardization, 2002, *Eurocode 1: Actions on Structures*, 2002.
- [7] General Service Administration(GSA), 2008, *Progressive Collapse Analysis and Design Guidelines for New Federal Office Buildings and Major Modernization Projects*, 2008.
- [8] Department of Defense, 2005, *Design of Buildings to Resist Progressive Collapse*, 2005.
- [9] JTG D65-01-2007, Guidelines for Design of Highway Cable-stayed Bridge.
- [10] HE X.H, LIU B. & LI Y. 2001. (The summary of design and construction of Shen Zheng northern station bridge. *East China Hingway*, 06), pp. 28-31.
- [11] CAI, J.G et al., 2012, Discussion on the progressive collapse analysis of long-span space structures. *Engineering mechanics*, 29(3), pp. 143-149.
- [12] WOLFF, M. & STAROSSEK, U., 2010. Cable-loss analyses and collapse behavior of cable-stayed bridges. IABMAS2010, *The Fifth International Conference on Bridge Maintenance, Safety and Management*, July 11-15, Philadelphia, USA.